

# Ocular Blood Flow Measurements and their Importance in Glaucoma and Age-Related Macular Degeneration

Hanna J. Garzosi MD<sup>1</sup>, Nir Shoham MD<sup>1</sup>, Hak Sung Chung MD PhD<sup>2</sup>, Larry Kagemann MS<sup>2</sup> and Alon Harris PhD<sup>2,3</sup>

<sup>1</sup>Department of Ophthalmology, HaEmek Medical Center, Afula, and Rappaport Faculty of Medicine, Technion-Israel Institute of Technology, Haifa, Israel; and <sup>2</sup>Glaucoma Research and Diagnostic Center, Department of Ophthalmology, and <sup>3</sup>Department of Physiology and Biophysics, Indiana University, Indianapolis, IN, USA

**Key words:** imaging, ocular hemodynamics, Doppler, glaucoma, age-related macular degeneration

*IMAJ 2001;3:443-448*

This review is intended to offer a grounding in some of the methods used to evaluate ocular hemodynamics in glaucoma and age-related macular degeneration, two of the most widespread causes of blindness in the industrialized world. The methods that will be discussed are scanning laser ophthalmoscopic angiography with fluorescein and indocyanine green dye, confocal scanning laser Doppler flowmetry, ocular pulse measurement, and color Doppler imaging. Other techniques are in use in this field, but those covered in this article are the ones of greatest contemporary interest.

## Blood flow assessment

### Scanning laser ophthalmoscopic angiography

The recent introduction of the scanning laser ophthalmoscope has vastly increased the capabilities of quantitative angiography. The SLO is free of many of the deficiencies of the longer established techniques of photographic and video angiography. In the SLO the incandescent light source is replaced by a low power scanning argon laser beam that affords better penetration of lens and corneal opacities. Overall retinal illumination is reduced and contrast is improved since the laser beam only illuminates a single spot on the retina at any moment.

The SLO exploits the confocal principle. Reflected light exits the eye through the pupil and must pass through an aperture at the exterior principal focus of the lens before reaching a solid-state detector. This detector generates a voltage that is determined by the intensity of incoming light. The detector voltage level, measured in real time, creates a standard video signal. Scattered light and light reflected from sources outside the focal plane cannot enter the confocal aperture. The aperture is fully open in angiography mode. The signal is generally passed through a video timer and then an S-VHS video recorder. The resulting images resemble those obtained with standard video angiography but the spatial resolution and contrast are much improved.

The SLO can be used for both fluorescein angiography and

indocyanine green angiography. A 488 nanometer (nm) argon blue laser with a 530 nm barrier filter is provided for fluorescein angiography, and a 790 nm infrared diode laser with an 830 nm barrier filter is installed for indocyanine green angiography.

### SLO angiography

Analysis of fluorescein angiograms can yield hemodynamic measurements such as arteriovenous passage time and mean dye velocity. Arteriovenous passage time, analogous to mean circulation time, can be estimated by noting the time between arrival of dye at the measuring point on the designated artery with that on a designated vein. Mean dye velocity can be calculated by placing a second measuring window at a known distance downstream on the artery from the first arterial measuring window. The dramatic increase in temporal resolution using scanning laser ophthalmoscopy as compared to earlier methods permits visualization of hyper- and hypo-fluorescent segments in the perifoveal and superficial optic nerve head capillary circulation. These dark and light segments are readily visible as they pass through the capillaries. Using an image analysis system it is possible to compute the velocity of the moving segments by measuring the distance they travel in a sequence of frames and dividing by the time taken to cover that distance.

### SLO indocyanine green angiography

The bulk of ocular blood flow is supplied mainly by the choroid. It is therefore important to have a method for the evaluation of the vasculature of this region. The application of ICG and SLO has overcome some of the limitations of fluorescein angiography in the study of choroidal blood [1]. The near infrared light used for scanning laser ICG angiography penetrates the pigmented layers of the retina much more efficiently than the shorter wavelength light used in fluorescein angiography. ICG's high affinity for plasma proteins is also advantageous. Within the circulation approximately 98% of the dye binds to plasma

SLO = scanning laser ophthalmoscope

ICG = indocyanine green

albumin or lipoprotein [2]. As a result, ICG diffuses slowly out of the fenestrated choriocapillaris – unlike fluorescein dye, which leaks very rapidly and severely impairs the delineation of choroidal detail. High resolution ICG images can now be produced by scanning laser ophthalmoscopy.

Indiana University's Glaucoma Research and Diagnostic Center has developed a new analysis technique for the quantification of choroidal ICG angiography using the SLO [3,4]. The entire 40° ICG angiogram is divided into a number of small regions, and dye-dilution curves are created for each region. Six locations on the image, each a 6° square, are identified for analysis [Figure 1]. The average brightness of the area contained in each box is computed for each frame of the angiogram. Area dye-dilution analysis identifies three parameters from the dye-dilution curves: 10% filling time, the slope of the curve, and maximum brightness [Figure 2]. The 10% filling time is the amount of time required to reach brightness 10% above baseline. This parameter describes the rapidity of filling in the early choroidal filling phase. Slope of the filling curve is calculated by noting the difference between the intensity at 10% filling and that at 90% filling, and dividing the difference by the number of frames during that time, where each frame represents a known time interval. This parameter represents the overall speed of blood flow as it enters the choroid.

#### Confocal scanning laser Doppler flowmetry

The confocal scanning laser Doppler flowmeter, or Heidelberg retinal flowmeter manufactured by Heidelberg Engineering GmbH, Heidelberg, Germany, combines a laser Doppler flowmeter with a confocal scanning laser tomograph. The instrument obtains images of a 2,560 x 640  $\mu\text{m}^2$  x 400  $\mu\text{m}$  deep region of the retina or optic nerve head with a measurement accuracy of 10  $\mu\text{m}$ . A 790 nm laser scans every line of the target at a line sampling rate of 4,000 Hz. Upon completion of the scan, the HRF computer performs a fast Fourier transforma-

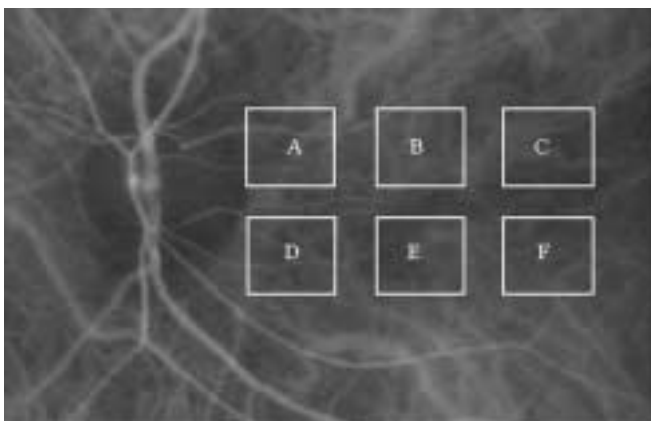


**Figure 1.** Forty degree indocyanine green choroidal angiogram using scanning laser ophthalmoscopy. Six locations on the image, each a 6° square, are identified for area dilution analysis: **A** and **D** for peripapillary choroid, and **B**, **C**, **E**, and **F** for macular area.

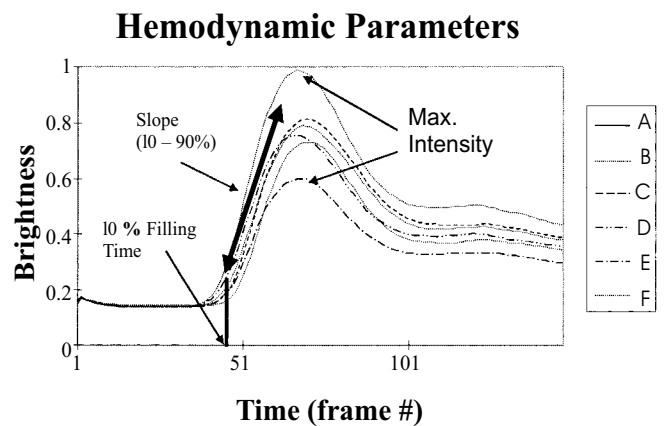


**Figure 2.** Hemodynamic parameters in area dilution analysis of indocyanine green choroidal angiography using scanning laser ophthalmoscopy. Area dye-dilution analysis identifies three parameters from the brightness maps: 10% filling time, the slope of each curve, and the maximum intensity of brightness. The 10% filling time is the amount of time required to reach a brightness 10% above baseline. The slope is the intensity difference between 10% and 90% filling divided by the time interval between them.

tion to extract the Doppler frequency shift of reflected light, point by point. A frequency spectrum is calculated for each point of the scan. Each frequency location on the X axis of the spectrum represents a blood velocity, and the height of the spectrum at that point is a function of the number of blood cells giving rise to the intensity of emission observed at that point. Integrating the spectrum yields a value for total blood flow. On its default setting the instrument analyzes a 10 x 10 pixel (100 x 100  $\mu\text{m}$ ) region of tissue.

The CSLDF has been shown to accurately measure blood flow in an artificial capillary tube ( $r=0.97$ ,  $P<0.0001$ ), and operators have obtained coefficients of reliability close to 0.85 for acutely repeated volume, velocity, and flow measurements from 10 x 10 pixel sampling areas [5]. Over a longer time, reproducibility from these small sampling boxes is inadequate; the coefficients of variation of measurements taken each week for 4 weeks have been shown to average 30% of the mean [6]. Furthermore, perfusion of the conventional/default 10 by 10 pixel area for data collection may not be representative of blood flow in the retina as a whole. To overcome these limitations, the Glaucoma Research and Diagnostic Center of Indiana University has developed a pixel-by-pixel analysis method [4,7], in which individual qualifying pixels from the entire 256 x 64 pixel image are examined [Figure 3]. Large vessels, peripapillary atrophic regions, and image areas interrupted by movement saccades are avoided. In processing the data the total number of pixels in the image is determined, an average flow value is

HRF = Heidelberg retinal flowmeter

CSLDF = confocal scanning laser Doppler flowmetry

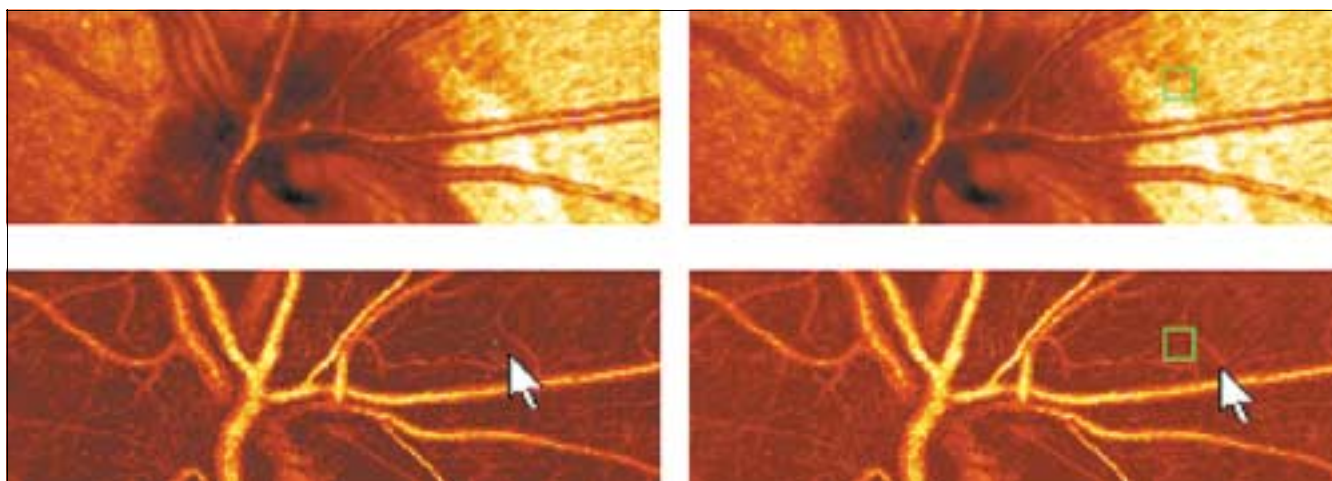


**Figure 3.** Confocal scanning laser Doppler flowmetry (Heidelberg retinal flowmeter) of optic nerve head and peripapillary retina. The left arrow indicates a 1 x 1 pixel measurement window, which collects flow values from the entire retina except for large vessels, for new pixel-by-pixel analysis. The right arrow indicates a 10 x 10 pixel measurement window used for conventional analysis.

calculated, and a histogram of flow data is produced. Flow, volume, and velocity data at the 25th, 50th, 75th, and 90th percentiles are the derived characteristics and are used for analysis. The percentage occurrence of zero flow pixels within the image is also calculated. Broadening the analysis to include every qualifying pixel within the entire image improves test/retest reliability, reducing the coefficient of variation for repeated weekly measurements to 15% for selected portions of the flow histogram.

### Ocular pulse measurement

In 1962 Eisenlohr and Langham [8] published the first study on the relationship between the observable pulsatile change in intraocular pressure during the cardiac cycle and the resulting changes in ocular volume. On the basis of his observations of the volume-pressure relationship, Langham developed the ocular blood flow device, which calculates the real-time change in ocular volume from real-time measurement of IOP [9]. Diastolic flow is the steady flow delivered during diastole, which accounts for perhaps two-thirds of total ocular flow. If pulsation in IOP is due to blood surging into the eye during systole, then it might be possible to measure an unknown percentage of total ocular blood flow in terms of IOP fluctuation.

The Langham OBF device consists of a modified pneumotonometer interfaced with a microcomputer that records the ocular pulse [10]. It monitors the rhythmic change in IOP during the cardiac cycle, which fluctuates within a range of up to 2 mmHg in a sinusoidal fashion. In the OBF examination procedure the tonometer is placed on the cornea for several seconds. The pneumotonometer sends an analog signal to the

computer, where it is digitized and recorded. The amplitude of the IOP pulse wave is used to calculate the change in ocular volume, using the relationship described by Silver et al. [11]. The OBF system (OBF Labs Ltd., Malmesbury, UK) has recently been introduced. Similar to the Langham ocular blood flow system, it has rapidly gained popularity for use in ocular blood flow studies because it is fast and straightforward in operation, easy to use, relatively inexpensive, and offers acceptable reproducibility [12].

Despite their attractiveness, both systems are beset by limitations. Pulsatile ocular blood flow values are not obtained through direct measurement of ocular blood flow, but derived mathematically by estimating ocular pulse volume change on the basis of a preset equation relating ocular volume to IOP. This formula incorporates a model of the cardiac cycle and a standard value for scleral rigidity. POBF measurements are therefore affected by individual differences of scleral rigidity, ocular volume, heart rate, systemic blood pressure, and IOP. This being the case, myopic eyes, which have less scleral rigidity and larger ocular volume, may yield lower POBF measurements than normal or hyperopic eyes. Understanding these limitations is essential to proper study design and data interpretation. POBF may be more useful for studying intra-individual blood flow changes (e.g., before and after medication) than for making inter-individual comparisons (e.g., glaucoma patients versus normal subjects).

### Color Doppler ultrasound imaging

A-scan ultrasound is commonly used to measure the eye's axial length, while B-scan ultrasound has been used for some years to produce grayscale images of ocular structures. Color Doppler

IOP = intraocular pressure  
OBF = ocular blood flow

POBF = pulsatile ocular blood flow

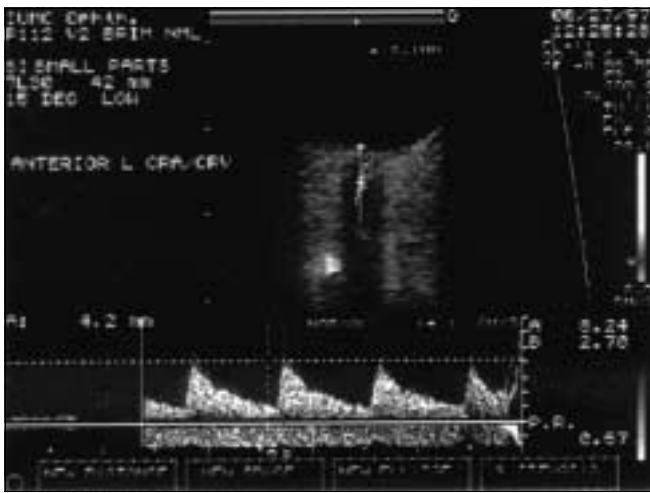


**Figure 4.** Color Doppler image of the central retinal artery and vein taken with a 7.5 MHz linear probe (Siemens Quantum 2000 system). The Doppler-shifted spectrum (time velocity curve) is displayed at the bottom of the image. Red and blue pixels represent blood movement towards and away from the transducer respectively.

imaging is an ultrasound technique that combines B-scan grayscale imaging of anatomical detail, color representation of blood flow as measured by Doppler shift, and pulsed Doppler measurement of blood flow velocities. As in the other Doppler-based methods, blood flow velocity is determined by the shift in the frequency of returning sound waves. The motion of blood through the vessels is represented by the superimposition of color upon the familiar B-scan grayscale image of the eye's structure. Most units code red-to-white for motion toward the probe and blue-to-white for motion away from the probe.

The color Doppler image [Figure 4] enables the operator to identify the target vessel and position the sampling window for pulsed Doppler recording. Measurements are of Doppler-shifted sound frequencies reflected by the tissue within the sampling window. The CDI unit plots flow velocity data against time, and the peak and trough of the wave are identified by the operator. From these, the computer calculates peak systolic velocity (PSV) and end-diastolic velocity (EDV). In addition, Pourcelot's resistive index – a measure of downstream vascular resistance – can be calculated according to the formula given below [13]:

$$RI = \frac{PSV - EDV}{PSV}$$

Values of this index range from zero to one, with higher values indicating higher distal vascular resistance.

*In vitro* studies have established the validity of Doppler ultrasound measures of flow velocity [14]. Reproducibility has also been studied [15]. The best reproducibility is found in the ophthalmic artery, where percentage coefficients of variation range from 4% for resistive index to 11% for peak systolic velocity.

### Ocular perfusion defects in glaucoma

Scanning laser ophthalmoscopic fluorescein angiography has provided important information on retinal hemodynamics in normal and glaucomatous subjects. Wolf and co-workers [16] used an SLO to measure retinal blood velocities of medically treated primary open-angle glaucoma patients and matched controls. They found an 11% reduction in the mean dye velocity within major retinal arteries in the glaucomatous group. In addition, arteriovenous passage time within the retina was 41% greater in the patients with primary open-angle glaucoma [16].

Scanning laser ophthalmoscopic ICG angiography has also been used to investigate ocular hemodynamics. In a recent study using a new area dilution analysis technique, ICG angiograms were recorded from 11 normal tension glaucoma patients and 12 age- and IOP-matched normal subjects [3]. There was no significant difference between the normal subjects and NTG patients in mean of slope, 10% filling time, or intensity of brightness, but the difference between maximum and minimum values in the six areas was significantly greater in the NTG patients. The difference in 10% filling time between the peripapillary and macular areas (mean of A and D vs. mean of B,C,E, and F in Figure 1, respectively) was also significantly greater in the NTG patients. It can thus be concluded that the pattern of early choroidal filling is homogeneous in normal subjects but heterogeneous in NTG patients. In addition, peripapillary choroidal filling was delayed in NTG patients but not in normal subjects. These findings suggest that NTG patients may suffer from hypoperfusion of the choroid.

In a recent study that used CSLDF in conjunction with a new pixel-by-pixel method of analysis described earlier, it was found that NTG patients presented with significantly lower blood flow than did age-matched normal subjects [4]. In histograms of flow data utilizing every pixel from the peripapillary retina, NTG patients had significantly lower flow in pixels at the 25th, 50th, and 75th percentiles of flow (each  $P < 0.05$ ) than did age-matched controls. Conventional CSLDF analysis using the instrument's default 10 x 10 pixel reading frame failed to distinguish between the two groups.

Glaucoma patients have been shown to have much lower pulsatile ocular blood flow than healthy subjects [10,17,18] or healthy ocular hypertensive subjects [19]. Several research groups have used CDI to assess orbital hemodynamics in glaucoma. Patients with primary open-angle glaucoma have been shown to have lower blood flow velocities in the

ophthalmic, central, and posterior ciliary arteries [20–22]. Another study found that patients with NTG had lower PSV than normal subjects in the ophthalmic and central retinal arteries [23]. Harris and co-workers [24] found that NTG patients had significantly lower EDV and higher resistance indices in the ophthalmic arteries compared with healthy controls at the baseline resting condition. Upon breathing carbon dioxide, a potent vasodilator, the parameters remained unchanged in healthy controls, while in glaucoma patients EDV increased and resistance indices decreased to the extent that the differences between the groups were abolished. It can be concluded from these results that NTG patients may be subject to reversible ocular vasospasm [24]. Galassi and co-workers [25] concluded that abnormalities in the ophthalmic artery blood flow systolic velocity, found by means of CDI, might be a vascular risk factor for the pathogenesis of the glaucomatous optic neuropathy, especially in patients with glaucoma associated with high myopia.

Color Doppler imaging is also useful for assessing the effect of newer drugs on ocular blood supply [26]. Martinez et al [26] found that PSV of the central retinal artery in glaucomatous eyes, and the EDV of the ophthalmic and central retinal arteries in both glaucomatous and normal eyes, were significantly higher after application of dorzolamide, a topical carbonic anhydrase inhibitor.

### Ocular perfusion defects in age-related macular degeneration

Delayed choroidal filling has been noted angiographically in patients with exudative AMD [27], and there is some evidence that choroidal blood flow is abnormal in patients with non-exudative AMD [28]. It is very difficult to quantify choroidal blood flow angiographically, since analysis is greatly complicated by the presence of the overlying retinal circulation and by the multi-layered nature of the choroidal circulation. The choroidal circulations of 12 healthy eyes and 16 non-exudative AMD eyes were compared using a new area dilution analysis technique, described earlier in its application to ICG angiography [4]. The mean 10% filling time and the range of 63% filling times were greater in AMD patients than in normal subjects. These results are an objective demonstration of the greater heterogeneity of filling and lower flow within the choriocapillaris of non-exudative AMD patients as compared to normal subjects.

Friedman and colleagues [29] found significantly lower flow velocities and resistive indices in the central retinal and posterior ciliary arteries in patients with AMD compared to controls. This study included a heterogeneous population of both exudative and non-exudative AMD patients. A recent study using CDI at Indiana University found that subjects with non-exudative AMD had significant vascular defects in the nasal and

temporal posterior ciliary arteries, which supply the choroid [30]. It can be concluded from this study that retrobulbar blood flow abnormalities are present in non-exudative AMD.

Although these studies lend some support to the postulated vascular pathogenesis of AMD, it is not yet possible to determine whether or not the abnormalities in choroidal perfusion play a causative role in non-exudative AMD, whether they are merely associated with another primary alteration (such as a primary retinal pigment epithelium defect or a genetic defect at the photoreceptor level), or whether they are more strongly associated with one particular form of this heterogeneous disease. Further study is warranted.

### Summary

This survey of methods for assessing ocular hemodynamics in glaucoma and age-related macular degeneration is not complete, but it does cover those likely to be encountered in the literature. A fundamental problem in getting to grips with the ocular blood flow literature is the difficulty in comparing the results of similar studies employing different assessment techniques. As evident from the discussion above, each technique evaluates a portion of the ocular circulation in a distinct way. Some of the methods overlap with regard to the tissues that can be used for examination, while others are directed at entirely different parts of the ocular vasculature.

Despite these difficulties, hemodynamic studies of glaucoma and AMD are likely to grow in importance. On the basis of accumulating epidemiological and clinical evidence, it is becoming apparent that intraocular pressure is not the sole etiological factor in glaucoma, and retinal pigment epithelium senescence is not the sole etiological factor in AMD. Circumstantial evidence of vascular involvement in glaucoma and AMD has now been bolstered by experimental evidence.

If the current pace of refinement of newly established technologies for evaluating ocular blood flow is maintained, they will soon be ready for deployment in the clinic. The only problem is the availability of expensive instruments and trained personnel. The ultimate beneficiaries of work in this area will not be researchers, but patients.

### References

1. Flower RW, Hochheimer BF. Clinical infrared absorption angiography of the choroid. *Am J Ophthalmol* 1972;73:458–9.
2. Cherrick GR, Stein SW, Leevy CM. Indocyanine green: observations on its physical properties, plasma decay, and hepatic extraction. *J Clin Invest* 1960;39:592.
3. Chung HS, Harris A, Kagemann L, Evans DW. Choroidal hemodynamics in normal tension glaucoma as assessed by a new analysis system. Second International Glaucoma Symposium, Jerusalem, Israel, 17 March 1998, p 41.
4. Chung HS, Harris A, Kagemann L, Martin B. Peripapillary retinal blood flow in normal tension glaucoma. *Br J Ophthalmol* 1999;83:466–9.
5. Michelson G, Schmauß B. Two-dimensional mapping of the perfusion of the retina and optic nerve head. *Br J Ophthalmol* 1995;79:1126–32.
6. Kagemann L, Harris A, Chung HS, Evans DW, Buck S, Martin B. Heidelberg retinal flowmetry: factors affecting blood flow measurement. *Br J Ophthalmol* 1998;82:131–6.

EDV = end-diastolic velocity

AMD = age-related macular degeneration

7. Harris A, Kagemann L, Evans D, Chung HS. A new method for evaluating ocular blood flow in glaucoma: Pointwise flow analysis of HRF images. *Invest Ophthalmol Vis Sci* 1997;38(Suppl):439.
8. Eisenlohr JE, Langham ME. The relationship between pressure and volume changes in living and dead rabbit eyes. *Invest Ophthalmol* 1962;1:63–77.
9. Langham ME. Ocular blood flow and visual loss in glaucomatous eyes. In: Krieglstein GK, ed. *Glaucoma Update III*. Berlin: Springer-Verlag, 1987:58–66.
10. Langham ME, Farrel R, Krakau T, Silver D. Ocular pulsatile blood flow, hypotensive drugs, and differential light sensitivity in glaucoma. In: Krieglstein GK, ed. *Glaucoma Update IV*. Berlin: Springer-Verlag, 1991:162–72.
11. Silver DM, Farrell RA, Langham ME, O'Brien V, Schilder P. Estimation of pulsatile ocular blood flow from intraocular pressure. *Acta Ophthalmologica* 1991;191(Suppl.):25–9.
12. Yang YC, Hulbert MFG, Batterbury M, Clearkin LG. Pulsatile ocular blood flow measurements in healthy eyes: reproducibility and reference values. *J Glaucoma* 1998;6:175–9.
13. Pourcelot L. Indications of Doppler's ultrasonography in the study of peripheral vessels. *Rev Prat* 1975;25:4671–80.
14. von-Bibra H, Stempfle HU, Poll A, Scherer M, Renner U, Moravec S, Bluml G, Blomer H. Accuracy of various Doppler techniques in recording blood flow velocity. *Studies in vitro*. *Z Kardiol* 1990;79:73–82.
15. Williamson TH, Harris A. Color Doppler imaging of the eye and orbit. *Surv Ophthalmol* 1996;40:255–67.
16. Wolf S, Arend O, Sponzel WE, Schulte K, Cantor LB, Reim M. Retinal hemodynamics using scanning laser ophthalmoscopy and hemorheology in chronic open-angle glaucoma. *Ophthalmology* 1993;100:1561–6.
17. Fontana L, Poinoosawmy D, Bunce CV, O'Brien C, Hitching RA. Pulsatile ocular blood flow investigation in asymmetric normal tension glaucoma and normal subjects. *Br J Ophthalmol* 1998;82:731–6.
18. Chiou HJ, Chou YH, Liu CJ, Hsu CC, Tiu CM, Teng MM, Chang CY. Evaluation of ocular arterial retinal changes in glaucoma with color Doppler ultrasonography. *J Ultrasound Med* 1999;18:295–302.
19. Trew DR, Smith SE. Postural studies in pulsatile ocular blood flow: II. Chronic open angle glaucoma. *Br J Ophthalmol* 1991;75:71–5.
20. Galassi F, Nuzzaci G, Sodi A, Casi P, Viello A. Color Doppler imaging in evaluation of optic nerve blood supply in normal and glaucomatous subjects. *Int Ophthalmol* 1992;16:273–6.
21. Königsreuther KA, Michelson G. Retinal hemodynamics in glaucoma. ARVO Abstract. *Invest Ophthalmol Vis Sci* 1994;35(Suppl):1842.
22. Sergott RC, Aburn NS, Tribble JR, Costa VP, Lieb WE, Flaharty PM. Color Doppler imaging: methodology and preliminary results in glaucoma. *Surv Ophthalmol* 1994;38(Suppl):S65–70. (Published erratum appears in *Surv Ophthalmol* 1994;39:165).
23. Durcan FJ, Flaharty PM, Digre KB, Lundergan MK. Use of color Doppler imaging to assess ocular blood flow in low tension glaucoma. ARVO Abstract. *Invest Ophthalmol Vis Sci* 1993;34(Suppl):1388.
24. Harris A, Sergott RC, Spaeth GL, Katz JL, Shoemaker JA, Martin BJ. Color Doppler analysis of ocular vessel blood velocity in normal tension glaucoma. *Am J Ophthalmol* 1994;118:642–9.
25. Galassi F, Sodi A, Ucci F, Harris A, Chung HS. Ocular hemodynamics in glaucoma associated with high myopia. *Int Ophthalmol* 1998;22:299–305.
26. Martinez A, Gonzalez F, Capeans C, Perez R, Sanchez Solario M. Dorzolamide effect on ocular blood flow. *Invest Ophthalmol Vis Sci* 1999;40:1270–5.
27. Boker T, Fang T, Steinmetz R. Refractive error and choroidal perfusion characteristics in patients with choroidal neovascularization and age-related macular degeneration. *Geriatr J Ophthalmol* 1993;2:10–13.
28. Zhao J, Frambach DA, Lee PP, Lee M, Lopez PF. Delayed macular choriocapillary circulation in age-related macular degeneration. *Int Ophthalmol* 1995;19:1–12.
29. Friedman E, Krupsky S, Lane AM, Oak SS, Freidman ES, Egan K. Ocular blood flow velocity in age-related macular degeneration. *Ophthalmology* 1995;102:640–6.
30. Ciulla TA, Harris A, Chung HS, Danis RP, Kagemann L, McNulty L, Pratt LM, Martin BJ. Color Doppler imaging discloses reduced ocular blood flow velocities in nonexudative age-related macular degeneration. *Am J Ophthalmol* 1999;128:75–80.

**Correspondence:** Dr. H.J. Garzozzi, Dept. of Ophthalmology, HaEmek Medical Center, Afula 18101, Israel. Phone/Fax: (972-4) 649-4397, email: garzozzi@clalit.org.il